

## A simulation-based study using boundary conditions of a thermal response for common building materials in a low-income housing for Kampala, Uganda

Ibrahim S. Madugu<sup>1</sup>, Madubuko C. Emeka<sup>\*2</sup>, Isah B. Yabo<sup>3</sup>, A. Abdulkarim<sup>3</sup>, Ibrahim M. Ribah<sup>5</sup>, Aisha L. Bagiwa<sup>5</sup>, Aminu U. Yabo<sup>6</sup>, Yinusa A. Adediran<sup>7</sup>, Benjamin J. Olufeagba<sup>7</sup>

<sup>1</sup>Directorate of ICT, Kampala International University, Uganda

<sup>2</sup>Georgetown Global Health Nigeria (GGHN), Abuja

<sup>2</sup>Department of Mathematics, Kampala International University, Uganda

<sup>3</sup>Directorate of Higher Degree, Kampala International University, Uganda

<sup>4</sup>Department of Biological and Environmental Sciences, Kampala International University, Uganda

<sup>5</sup>Department of Basic Science, Shehu Shagari University of Education, Sokoto, Nigeria

<sup>6</sup>Department of Electrical and Electronics Engineering, University of Ilorin, Nigeria

Corresponding author: e-mail: em1425@georgetown.edu

### Abstract

Indoor thermal comfort is still a major issue in low-income housing in tropical urban areas like Kampala, Uganda, where passive design techniques are frequently the only practical way to manage heat. A boundary-condition-based thermal simulation of popular building materials, such as concrete walls, plastered brick walls, thatch roofing, and dark and light-colored metal roofs, is shown in this paper. Monthly surface temperature rise ( $\Delta T_{material}$ ) and indoor air temperature rise ( $\Delta T_{atr}$ ) were calculated over the monthly average sun exposure duration using local climatic data, which included solar irradiance, wind speed, and ambient air characteristics. According to the results, light-colored metal roofs minimise surface heating by more than 60%, while dark-coloured metal roofs create significant heat gain ( $\Delta T_{material} > 10,000$  °C under simplified models). Thatch roofs performed better thermally because of their large heat capacity and low thermal conductivity. Thermal inertia from concrete and brick walls hinders heat transport and could cause discomfort at night if ventilation is inadequate. For reasonably priced tropical homes, the study emphasises the necessity of careful material selection and colour adaptation in passive thermal design. These observations help East African cities make evidence-based decisions on sustainable building, architectural design, and housing policy.

**Keywords:** building materials, solar radiation, absorption energy, boundary conditions

## 1. Introduction

The Sun provides nearly all of the Earth's energy, maintaining a suitable temperature for life, generating solar power, and influencing weather patterns. This sunlight reaching the Earth's surface is absorbed by land surfaces, oceans and atmosphere at an average of 340 watts per square metre and converted into different forms such as heat (thermal energy), electrical energy (in solar

cells), fuels evaporation, or chemical energy (via photosynthesis) (Nafees, 2024). Albedo is the ratio of the light that a surface reflects compared to the total incoming sunlight. A surface that reflects all the light has an albedo equal to one, while a surface that reflects 40% of the light has an albedo level of 0.4 (Nafees, 2024). Thus, the surface type, such as the Earth's surface albedo, which comprises the atmosphere, land surfaces, and oceans, determines how much of the incoming solar energy is reflected into space.

Instead of absorbing and converting incoming shortwave solar radiation—mostly visible and near-infrared light—into heat, high-albedo materials reflect a sizable amount of this energy into the atmosphere and eventually into space. The majority of the reflected radiation returns through the atmosphere after bouncing off the Earth's surface. Most of it escapes into space, contributing to the Earth's planetary albedo, while some is dispersed by clouds, aerosols, or gases, such as water vapour, as shown in Figure 1. On both a local and global level, this is net cooling (K. W. Oleson, 2010). Some of this energy is scattered and reabsorbed by aerosols and clouds in the lower atmosphere, resulting in a slight heating of the atmosphere; however, this is less than what would be absorbed had the radiation hit a low-albedo surface (Masson-Delmotte, 2021).

The Earth's climate change is determined by the albedo, as a decrease in albedo increases the absorption of energy, hence the Earth gets warmer. The Earth's energy balance requires the average albedo to be around 0.3, meaning that the Earth reflects into space 30% of light and absorbs 70%. Albedo keeps changing at different seasons or at different times of the day. It also depends on the type – planetary albedo or bond albedo is the total reflectivity of Earth with contributions from clouds, oceans, ice, and land; surface albedo is the reflectivity of ground/ocean surface from fresh snow, forest, ocean, urban areas and spectral albedo that is reflectivity at specific wavelengths.

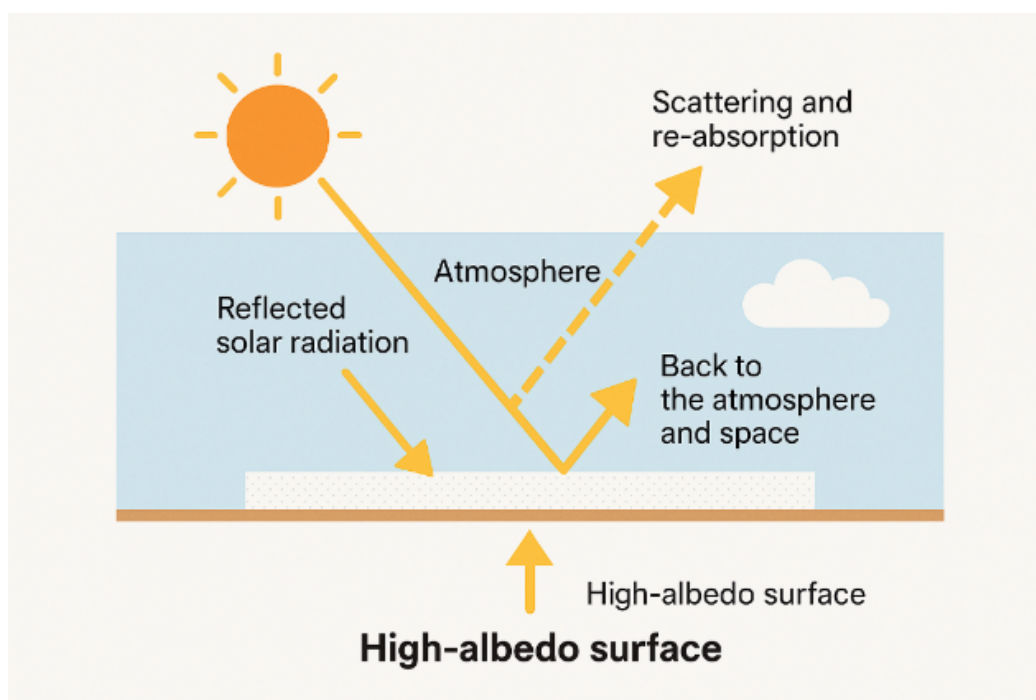


Fig. 1: High-albedo Surface showing Reflection and Absorption.

There are various contributors to albedo control/changes, including clouds, ice and snow, land use, ocean colour, and aerosol. Anthropogenic interferences, especially to land usage such as urbanisation due to an increase in population, industrialisation, and other economic developments, affect the climate and change the albedo (Xu, Gregory, & Kirchain, 2015). Also, urban areas are characterised by high carbon emission that has long-term effects on the climate. Thus, increasing the global surface albedo, especially the urban areas, which offsets radiative forcing from carbon dioxide (CO<sub>2</sub>) and aerosols, can help fight climate change. High-albedo or cool roofs could shrink future CO<sub>2</sub> emissions due to fossil fuel electricity generation used for air conditioning and refrigeration (Elise Stull, 2010).

The global urban areas coverage of roadways, buildings, and rooftops is 75% in high-density, 70% in medium-density, and 65% in low-density areas. Most of the urban settlements in the United States of America for example have surface coverage for roofs and pavements of an average of

23% and 35%, respectively (Xu, Gregory, & Kirchain, 2015). Therefore, to increase the albedo, the roofs are changed every two to three decades while roadways are resurfaced every 10 years. In many states in the US, policies are designed to encourage cool roof installations for energy use reduction, increase air quality, and mitigate the urban heat island effect (Xu, Gregory, & Kirchain, 2015).

The Urban Heat Island (UHI) is a phenomenon where urban and semi-urban settlements are known to have elevated temperatures in comparison to surrounding rural areas. This is due to higher demand for energy, congestion, waste, and pollution. UHI exacerbates further demand for energy for cooling homes and offices, increases air pollution, and poses health risks. The use of high-albedo materials, especially on rooftops and the painting of structures, helps in reflecting a significant portion of the incoming solar radiation and reducing heat absorption. Kampala, Uganda, is the focus of this study to assess the role of high-albedo surfaces in climate change adaptation.

Several design techniques have been put out to reduce the amount of heat that urban dwellers are exposed to. Among these are cooling centres, wind corridors, and anthropogenic heat emission reductions. Using high-albedo surfaces to regulate the transformation and interchange of incoming solar radiation is one of the more efficient ways to lower the surface temperature of urban areas (Ian A. Smith, 2022). Some of the reflected radiation can strike adjacent buildings, trees, or vehicles, causing radiative exchange or secondary heating, however, the net energy gain is still lower than that of heat absorbed by dark surfaces (Taha, 1997).

## **2. Benefits of High-Albedo Surfaces**

By reflecting more sunlight and absorbing less heat, high-albedo materials—like reflective pavement and roofing—have been used to reduce excessive urban heat. By using these materials,

metropolitan areas can become cooler, less energy is used for cooling, and outdoor thermal comfort can increase (Ian A. Smith, 2022).

The albedo of a surface is its hemispherical and wavelength-integrated reflectance for both heterogeneous and complicated surfaces, as well as basic uniform surfaces (Taha, 1997). Urban albedos typically fall between 0.10 and 0.20, while some cities may have higher values. While most US and European cities have lower albedos (0.15 to 0.20), North African towns are excellent instances of high albedo urbanised areas (albedos of 0.30 to 0.45). Furthermore, it is discovered that the majority of urbanised basins have albedo values between 0.12 and 0.16, with the city core's albedo being higher than that of its surroundings, in part due to the latter's more widespread vegetation (Taha, 1997). Urban albedo significantly varies across cities due to building materials, vegetation cover, and geographical location. In Figure 2, albedo values from some selected cities worldwide are shown:

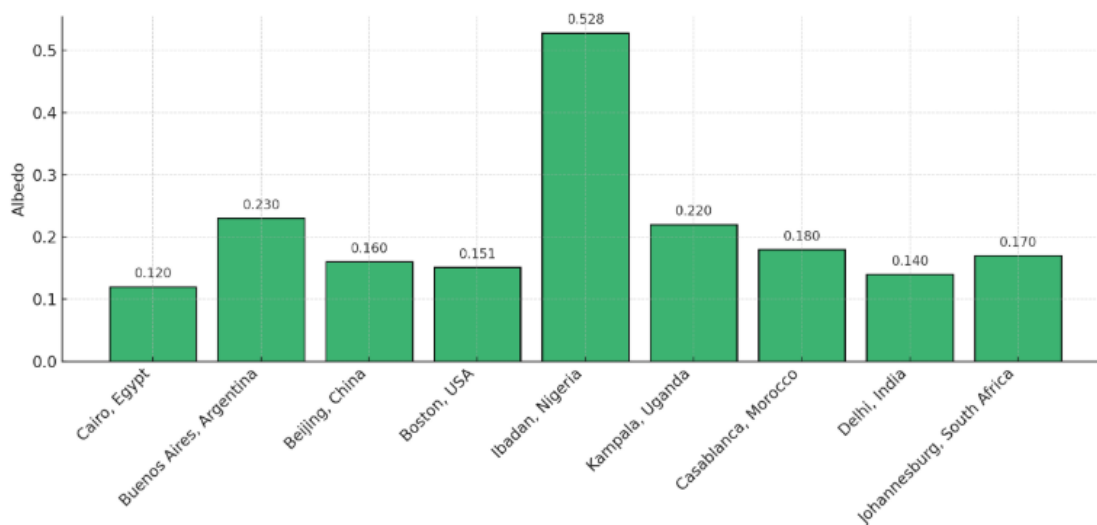


Fig. 2: Urban Albedo Values in Selected Cities Worldwide (Taha, 1997) (A. Trlica1, 2017) (K. W. Oleson, 2010) (Lei, 2019).

### 3. Data and Method

#### 3.1 Study Area

Uganda is a country in Africa (Eastern Africa) covering a total area of 241,038 km<sup>2</sup> (Kilama, 2014) with a population of 45,905,417, with a population density of 190 persons/Km<sup>2</sup> (UBOS, 2024). The country lies along the equator with a climate that exhibits two main seasons (wet and dry season). Uganda’s housing and living condition shows that 81.1% and 53.4% of the households have access to improved water and electricity, respectively (UBOS, 2024).

Kampala is the capital of Uganda (Figure 3) and the seat of government. It lies within the coordinates of 0°18' 49" N, 32° 34' 52" E. The city borders Lake Victoria in the East, Wakiso District in the West, and the North. Kampala has the highest daytime population of 2,503,175 persons in Uganda. However, the total major population of Kampala is around 1.7 million people. There are 529,057 households in Kampala, averaging 2.9 persons per house.

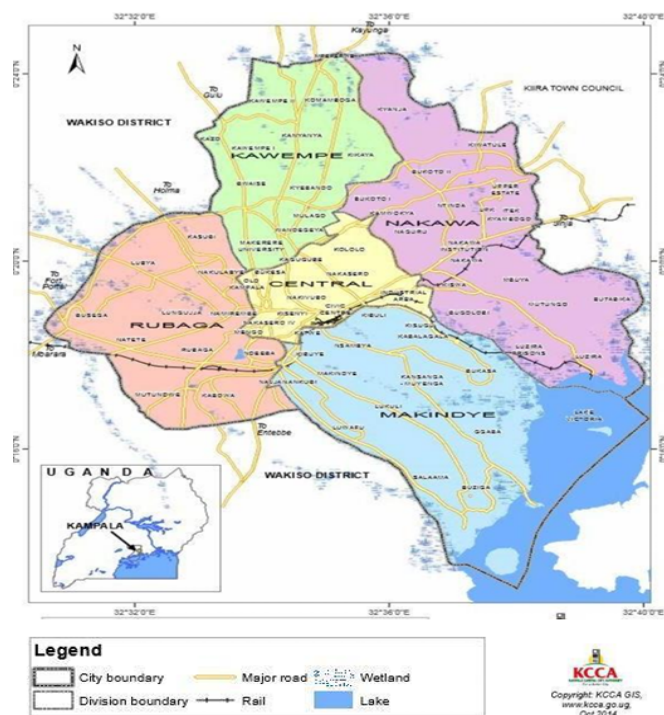


Fig. 3: Map of Kampala by Divisions (KCA, 2025)

## 3.2 Kampala Climate Profile

Kampala is situated near the equator, covering an area of 195 km<sup>2</sup> (the Kampala region (greater Kampala) covers an estimated land area of 1,895 km<sup>2</sup>) at a latitude of 0.35°N, with high solar insolation throughout at an average irradiance between 5.5 and 6.0 kWh/m<sup>2</sup>/day. The ambient temperatures are typically between 18°C and 30°C. Being close to the equator, the region ought to experience an equatorial climate, yet due to its high altitude and the impact of Lake Victoria, the city experiences a tropical climate. The terrain has an average altitude of 1,120m above sea level and valleys covered by wetlands (KCA, 2025). In Table 1, the monthly climate overview of Kampala is shown.

Table 1: The Climate Overview Data of Kampala (Climechart, 2024) (NomadSeason, 2024), (Biira, 2014), (Africa, 2023).

Month	Temperature °C	Average Daily Insolation (kWh/m <sup>2</sup> /day)	Sunshine (h)	Snow (mm)
January	21.8	5.60	10.55	0.00
February	22.5	5.88	10.57	0.00
March	22.0	5.81	9.74	0.00
April	21.2	5.31	8.40	0.00
May	20.9	5.02	9.61	0.00
June	20.6	4.84	10.24	0.00
July	20.5	4.90	10.51	0.00
August	20.5	5.16	10.24	0.00
September	20.8	5.57	10.23	0.00

Month	Temperature °C	Average Daily Insolation (kWh/m <sup>2</sup> /day)	Sunshine (h)	Snow (mm)
October	21.0	5.43	9.55	0.00
November	20.8	5.28	9.05	0.00
December	21.1	5.44	9.98	0.00

### 3.2.1 Solar Radiation

It can be seen from Table 1, Kampala has 8 hours of average daily sunshine hours with an average daily insolation of approximately 5.2 kWh/m<sup>2</sup>/day, and the city receives significant solar radiation all year (Biira, 2014). Annually, there is about a 20% variation in solar radiation between 4.5 and 5.5 kWh/m<sup>2</sup>/day. (Africa, 2023). The solar radiation is highest during the equinoxes, in particular March and September, and the lowest periods occur between June and July due to cloud cover (Daniel N Katongole, 2023).

### 3.2.2 Temperature

The average monthly temperatures of Kampala are approximately between 20.5°C and 22.5°C, as shown in Table 1. The months of January, February, and March recorded the warmest daily mean temperatures of 23°C, while July, August, and September have the coldest temperatures of a daily mean of 22°C (NomadSeason, 2024).

### 3.2.3 Rainfall

The rainfall in Kampala is distributed unevenly throughout the year, with wetter months typically occurring from March to May and September to November, while July is the driest (Figure 4). This data is useful for seasonal planning in roofing material simulations, especially for evaluating water resistance and thermal performance.

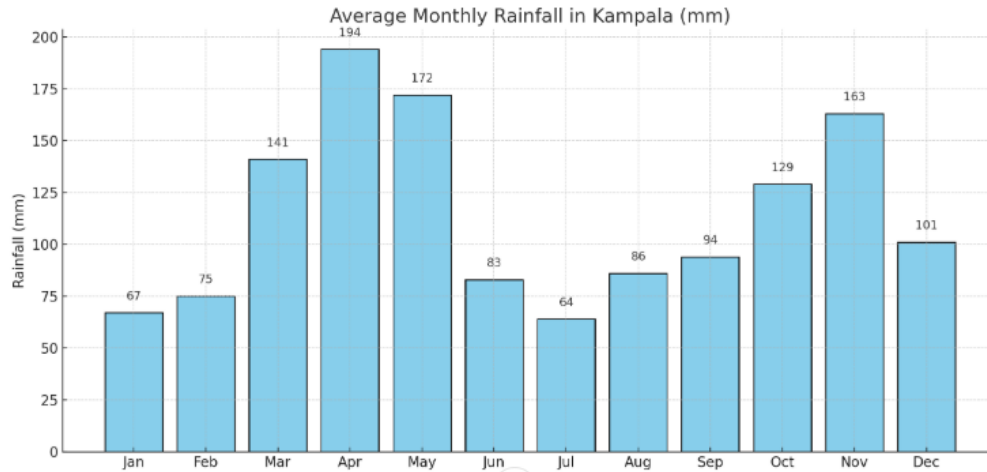


Fig. 4: Kampala Monthly Rainfall Distribution

## 3.4 Models

### 3.4.1 General Model for Solar Radiation Reflection

The mathematical model for solar radiation reflection from a 1 m<sup>2</sup> surface and considering the albedo of different surfaces, is defined as:

$$R = \alpha \cdot Q_{solar} \quad (1)$$

where  $R$  is the reflected solar radiation in W/m<sup>2</sup>;  $\alpha$  is the Albedo (reflectivity) of the surface (dimensionless, between 0 and 1), and  $Q_{solar}$  is the incoming solar radiation (W/m<sup>2</sup>), which depends on location, time, and atmospheric conditions.

It can be observed from equation (1) that there is a need to choose the right colours for a surface, as this will ensure the surface energy balance. The Albedo  $\alpha$ , for some selected common surface colours, is given as:

- White surface:  $\alpha \approx 0.80 - 0.90$
- Black surface:  $\alpha \approx 0.05 - 0.10$
- Grey surface:  $\alpha \approx 0.20 - 0.50$
- Red surface:  $\alpha \approx 0.30 - 0.50$

- Green surface:  $\alpha \approx 0.25 - 0.40$
- Blue surface:  $\alpha \approx 0.20 - 0.35$
- New thatch:  $\alpha \approx 0.30 - 0.35$
- Weathered thatch:  $\alpha \approx 0.20 - 0.25$

The solar radiation is not constant throughout the day as it depends on time and the weather variables of the location. Thus, the general expression for the incoming solar radiation,  $Q_{solar}$ , is given by:

$$Q_{solar} = Q_0 \cdot Q_t \cdot Q_w \cdot Q_L \quad (2)$$

where  $Q_0$  is the maximum direct solar irradiance (approximately  $800\text{W/m}^2$  at noon, direct sunlight);  $Q_t$  is the fraction of maximum sunlight based on time of day (ranges 0–1);  $Q_w$  is the atmospheric condition (weather/cloud) factor (ranges 0–1) and  $Q_L$  is the latitude correction factor (ranges 0–1)

From equations (1) and (2), a general model to estimate the reflection from any surface colour by adjusting albedo,  $\alpha$ , and local sunlight conditions is given in the form:

$$R_{surface} = \alpha_{surface} \times Q_0 \cdot Q_t \cdot Q_w \cdot Q_L \quad (3)$$

### 3.4.2 Mathematical Model for Solar Radiation Reflection in Building Materials

When considering building materials, the model has to be refined to include:

1. Material-specific albedo (reflectivity).
2. Material thermal absorption (some energy is absorbed and re-emitted as heat).
3. Surface roughness and texture, which affect scattering.

4. The angle of incidence of sunlight, as buildings receive solar radiation at different angles throughout the day.

Thus, the final reflected radiation equation is given by:

$$R_{surface} = \alpha_{surface} \times Q_o \times Q_t \times Q_w \times Q_L \times \cos(\theta) \quad (4)$$

where  $\theta$  is the solar incidence angle (angle between sunlight and the surface normal).

The albedo  $\alpha$ , for common building materials, is given in Table 2.

Table 2: Albedo for Common Building Materials

Material	Albedo ( $\alpha$ )
White Paint	0.75 – 0.90
Light-Colored Concrete	0.50 – 0.70
Dark-Colored Concrete	0.10 – 0.35
Asphalt	0.05 – 0.15
Brick (Red)	0.20 – 0.40
Glass (Reflective)	0.20 – 0.60
Green Roof (Vegetation)	0.25 – 0.40

### 3.4.3 Heat Absorption Factor

Not all of the solar energy is reflected; some is absorbed and contributes to the building's heat gain.

Thus, the absorbed energy is defined as:

$$Q_{abs} = (1 - \alpha) \cdot Q_{solar} \quad (5)$$

This model can be applied to:

- Building Cooling Design: Choose high-albedo materials for roofs and walls to reduce cooling costs.
- Urban Heat Island Mitigation: Using reflective materials in cities can lower ambient temperatures.
- Solar Panel Placement: Understanding reflection helps optimise solar panel efficiency.

### 3.4.4 Model for the Solar Radiation Reflection and Heat Absorption Energies

The study area (Kampala, Uganda) is a tropical region near the equator that involves several variables related to climate, material properties, and surface characteristics, particularly the colour of the surface. The climate condition models that evaluate the absorbed heat and reflected energy due to the incident solar radiation on the building surface and its exposure time to the solar incident consider the solar radiation input model, the models for the reflection and absorption, and the heat transfer into the material.

The total solar radiation on the building surface based on solar incident upon it and time of exposure is given by:

$$Q_{total} = Q_{solar} \times A_{total} \times t \quad (6)$$

where  $Q_{solar}$  is the solar irradiance in  $W/m^2$ ,  $A_{total}$  is the exposed surface area of the building to the sunlight in  $m^2$  (this is the total area for the roofing and walls, less openings for openings – windows and doors), and  $t$  is the time of exposure in seconds.

The reflection and absorption models are the energies that show the reflection and absorption of surfaces. These are defined as:

$$Q_{ref} = \alpha \times Q_{total} \quad (7)$$

and;

$$Q_{abs} = (1 - \alpha) \times Q_{total} \quad (8)$$

The major properties in calculating the reflection and absorption for any material consider the fraction of the solar energy reflected as the albedo (where it is 0 for total absorption of sunlight and 1 for total reflection), thermal conductivity, which is the rate at which the material conducts heat (W/m.K), the material's ability to store heat or heat capacity (J/kg.K), and the density of the material (kg/m<sup>3</sup>).

The heat transfer into a material is the heat conducted into (that penetrates the material) and out of the building (through windows and other openings) over some time. The heat flux in W/m<sup>2</sup> is the model for the heat transfer into a material defined by Fourier's law as:

$$q = \frac{k \cdot \Delta T}{L} \quad (9)$$

Where  $k$  is the thermal conductivity,  $\Delta T$  is the temperature gradient in °C or K, and  $L$  is the thickness in  $m$  of the material.

The temperature is not a constant variable due to the intermittent solar radiation. Thus, the rate of temperature change of the material is given by:

$$\frac{dT}{dt} = \frac{Q_{abs}}{m \cdot c} \quad (10)$$

where  $c$  is the heat capacity and  $m$  is the mass in kg of the material that is defined by:

$$m = A \cdot L \cdot \rho \quad (11)$$

## 3.4.5 Optimal Approach to the Solar Radiation Reflection and Heat

### Absorption Model

Optimising the models for the solar reflection and heat absorption for the study area (a tropical climate) entails balancing the thermal comfort, energy efficiency, and material cost. The optimised model considers the best selections for material, colour, and structural designs.

Some of the considerations for the optimal method are:

- High reflectivity to minimise heat absorption.
- Material durability and cost-effectiveness.
- Climate-specific adaptations (winter vs. summer).
- Thermal emissivity (how efficiently a material releases absorbed heat).

The objectives for the optimised system are to minimise the internal temperature rise  $\Delta T$  and the cooling load  $Q_{load}$ . This can be achieved after the consideration of internal heat gain and heat losses due to convection and radiation.

1. Internal Heat Gain: The internal heat gain is the heat generated from various sources that include:
  - Solar on roof and walls: This heat depends on the type of material and colours. For example, it is high for metals and dark colours.
  - Windows (glass gain): This is usually medium-high internal heat, but can be lowered by treated or tinted glasses.
  - People and devices: This is a medium internal heat gain from humans' body temperature and appliances in use at home.

- Air leakages or ventilation: This can vary due to climate conditions (especially atmospheric)

Therefore, for optimal purposes, the internal heat gain is considered as:

$$Q_{internal} = \sum(\text{watts per source} * t) \quad (12)$$

Optimising with heat gain entails the reduction of absorptivity through using light colours and reflective surfaces; increasing insulation (i.e, resisting conductive gain); releasing the trapped heat via smart ventilation and cooling due to shade. Thus, plugging the internal heat gain can be achieved as:

Step 1: Calculate the heat flow through the wall or roof that gives the rate of flow into the interior of the building and is defined by:

$$q = \frac{k * A * \Delta T}{L} \quad (13)$$

Step 2: The air temperature rise inside the building is given by the temperature rise of the air inside the house due to heat conducted through the material (roof/wall) into the house (rooms), given by:

$$\Delta T_{air} = \frac{q * t}{m_{air} C_{air}} = \frac{Q_{into\ room}}{m_{air} C_{air}} \quad (14)$$

where  $m_{air}$  is the mass of air given as:

$$m_{air} = \rho_{air} * V \quad (15)$$

The heat specific heat capacity for air  $C_{air}$  is approximated as 1005 J/kg.°C.

Step 3: The temperature rise of the building material's surface due to absorbed solar energy is given by:

$$\Delta T_{material} = \frac{Q_{abs}}{m.c} \quad (16)$$

2. Heat Losses: In practice, material loses heat after it absorbs heat. The heat losses are the convection (to the surrounding air) and radiation (to the sky or surrounding environment).

The net heat gain is therefore found from:

$$Q_{net} = Q_{abs} - Q_{conv} - Q_{rad} \quad (17)$$

The convective heat loss is the loss of heat due to the transfer of heat from the building material to the surrounding air and is defined by:

$$Q_{conv} = h * A * \Delta T_{material} * t \quad (18)$$

where  $h$  is the convective heat transfer coefficient ( $\text{W}/\text{m}^2\cdot\text{K}$ ).

This absorbed energy will give rise to the building's total internal temperature and is defined as:

$$Q_{rad} = \varepsilon * \sigma * A * (T_{material}^4 - T_{ambient}^4) \quad (19)$$

where  $\varepsilon$  is the emissivity (0.9 for most surfaces);  $\sigma$  is the Stefan-Boltzmann constant ( $5.6 \times 10^{-8} \text{W}/\text{m}^2\cdot\text{K}^4$ ) and  $T$  is the absolute temperature (Kelvin).

The temperature is defined by:

$$T_{material} = \Delta T + T_{ambient} \quad (20)$$

and

$$T_{ambient} \approx 298\text{K} (25^\circ\text{C}) \quad (21)$$

3. The implementation strategies of the optimisation model are:

- i. Calculate the absorbed energy  $Q_{abs}$
- ii. Assume an initial estimate of  $\Delta T$
- iii. Compute  $Q_{conv}$  and  $Q_{rad}$

- iv. Subtract from  $Q_{abs}$  to get  $Q_{net}$
- v. Recalculate  $\Delta T$  from  $\Delta T = \frac{Q_{net}}{m.c}$
- vi. Perform iteration until convergence is achieved for better precision.

### 3.4.6 Boundary Condition Approach

The boundary conditions allow the consideration of interaction between the material and environment, factoring in heat exchange across surfaces.

#### 1. Heat Transfer with Boundary Conditions

The heat transfer equations with the boundary conditions are modelled for the temperature distribution in materials using Fourier's law for heat conduction, Newton's law of cooling, and Stefan-Boltzmann's law for radiation. Thus, the general heat transfer equation in steady-state for a material exposed to solar radiation is defined by:

$$Q_{abs} = Q_{solar} * A * (1 - \alpha) * t \quad (22)$$

For heat conduction, it is defined as:

$$\frac{\partial^2 T(x)}{\partial x^2} = \frac{Q_{net}}{k * A} \quad (23)$$

where  $T(x)$  is the temperature at any point along the material's thickness.

The boundary conditions are given as follows:

- At the top surface (exposed to solar radiation):  $T_1 = T_{ambient} + \Delta T_{material}$
- At the bottom surface (interface with room or internal side):  $T_2 = T_{air}$

The equation for the temperature change can be solved numerically using finite difference methods or the finite element method for more complex scenarios.

## 2. Convection and Radiation Boundary Conditions

The material's surface has heat losses through:

- i. Convective heat loss  $Q_{conv}$ , this is defined as:

$$Q_{conv} = h * A * (T_{surface} - T_{ambient}) * t \quad (24)$$

- ii. Radiative heat loss,  $Q_{rad}$ , is defined by:

$$Q_{rad} = \varepsilon * \sigma * A * (T_{surface} - T_{ambient}) * t \quad (25)$$

These heat fluxes can be combined when considering the steady-state condition at a point where the heat absorbed is equal to the heat lost.

The merits of adding the boundary conditions to the optimised models make it easier to:

- Implement the finite difference methods or finite element analysis for the heat transfer across material layers
- Adjust parameters for the materials such as thickness, thermal properties, and the boundary conditions to minimise the temperature rise for comfort or energy efficiency. The system can support optimisation algorithms (e.g., genetic algorithms, gradient descent, etc).

For implementation purposes, a Python Simulation code is created that models the heat transfer variables for various building materials in Table 3 using boundary conditions and an optimisation algorithm to minimise temperature rise to achieve the best optimisation goal listed in Table 4.

Table 3: Heat Transfer Parameters for Various Building Materials

Property	Metal Roof	Concrete Wall	Brick Wall (Plastered)	Thatch Roof
----------	------------	---------------	---------------------------	-------------

<b>Albedo</b>	0.25 (dark)	0.35	0.45	0.15 (dark thatch)
<b>Thermal Conductivity (k)</b>	205 W/m·K	1.4 W/m·K	0.7 W/m·K	0.05 W/m·K
<b>Density (ρ)</b>	2700 kg/m <sup>3</sup>	2400 kg/m <sup>3</sup>	1800 kg/m <sup>3</sup>	400 kg/m <sup>3</sup>
<b>Specific Heat Capacity (c)</b>	900 J/kg·°C	880 J/kg·°C	840 J/kg·°C	1700 J/kg·°C
<b>Typical Thickness</b>	0.0005 m (0.5 mm)	0.15 m (150 mm)	0.2 m (200 mm)	0.15 m (150 mm)
<b>Emissivity</b>	0.90	0.85	0.90	0.95
<b>Area (Example)</b>	40 m <sup>2</sup>	40 m <sup>2</sup>	40 m <sup>2</sup>	40 m <sup>2</sup>
<b>Solar Irradiance</b>	800 W/m <sup>2</sup> (average)	800 W/m <sup>2</sup>	800 W/m <sup>2</sup>	800 W/m <sup>2</sup>
<b>Ambient Temperature</b>	25°C	25°C	25°C	25°C
<b>Convective Coefficient (h)</b>	15 W/m <sup>2</sup> ·K (natural conv.)	15 W/m <sup>2</sup> ·K	15 W/m <sup>2</sup> ·K	15 W/m <sup>2</sup> ·K

The plan and the code structure are as follows:

1. Simulation Setup: This involves defining the material's thermal properties (conductivity, density, specific heat); using the solar irradiance data and selecting appropriate building parameters and defining the boundary conditions for the material's surface ambient and air temperatures

2. Numerical Method (Finite Difference/Iterative Method): This allows the use of the heat conduction equation for a steady-state solution; calculating the temperature difference considering all heat loss mechanisms and optimising the material parameters for minimal temperature rise.
3. Optimisation: The simulation code uses a gradient descent to adjust the material properties and minimise the temperature difference.

Table 4: Optimisation Goals

Variable	Optimisation Goal	Target Value
Albedo (Roof)	Maximise	$\geq 0.7$
Albedo (wall)	Moderate	0.4 – 0.6
Thermal conductivity	Minimise for walls	$< 0.8$ W/m.K
Heat capacity	Maximise thermal mass	$\geq 1000$ J/kg.K
Temperature rise, $\Delta T$	Maximise	$\leq 5^\circ\text{C}$ from ambient

## 4.0 Results

### 4.1 General Models Validation

The solar radiation reflection for different roof types at direct sunlight ( $800\text{W}/\text{m}^2$ ) in Figure 5 shows that roof tops with brighter colours have the highest reflectivity values, while the darker ones reflect less energy. It can be seen that a white roofing material, such as zinc, has the highest reflected energy at  $680\text{W}/\text{m}^2$ , while black rooftops have the lowest reflection at  $60\text{W}/\text{m}^2$ . In between these extremes are the thatched rooftops that are common, especially in some rural

settlements, but very rare in Kampala. Observing their veracity can help in design purposes, as they seem to have significance.

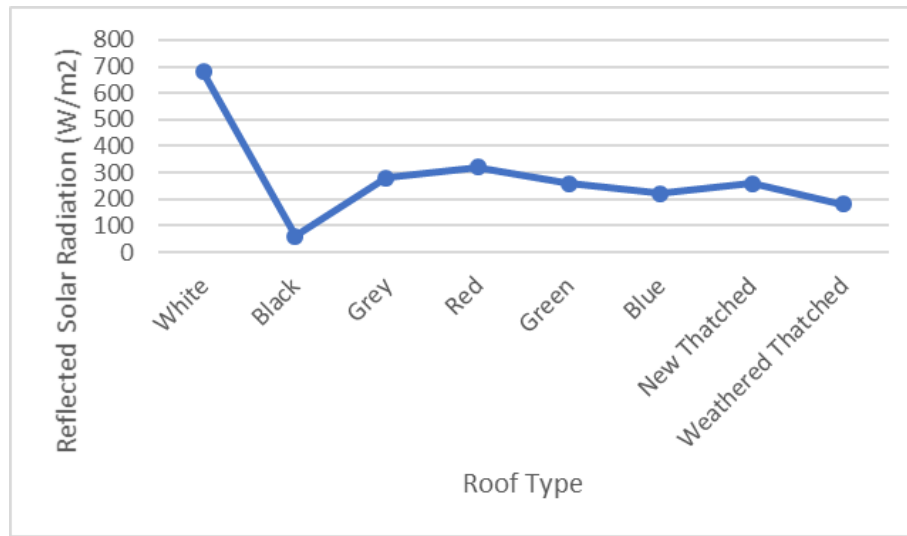


Fig. 5: Solar Radiation Reflection for Direct Sunlight for Different Rooftops

The reflection of different building materials at different sun positions (solar incidence angles) is presented in Figure 6. It can be observed that red brick (most of the buildings in Kampala are made up of red bricks) reflects a mid-value between brighter and darker coloured materials.

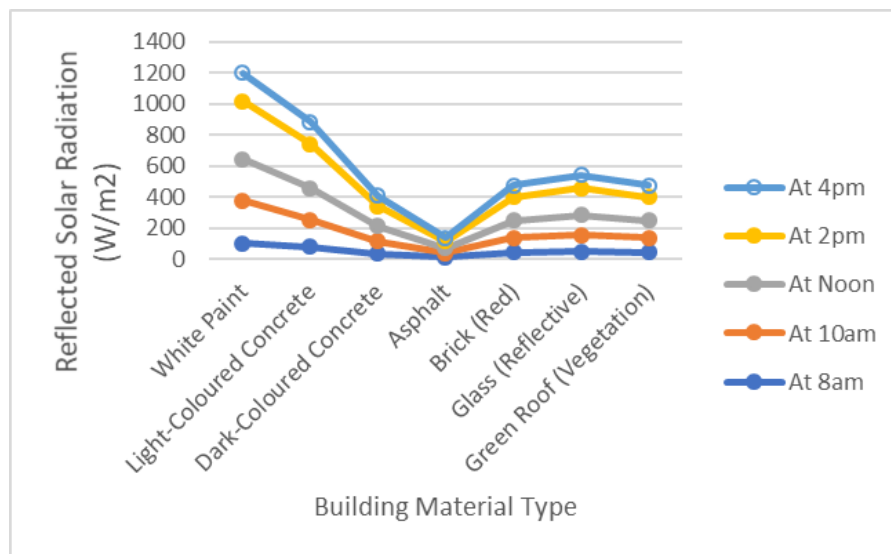


Fig. 6: Solar Radiation Reflection for Different Building Materials Surfaces at Different Times of the Day and Solar Incidence Angles

## 4.2 Solar Radiation Reflection and Heat Absorption Energies

In Figures 7 and 8, the heat absorption for different rooftops and building materials is presented. It can be seen that surfaces with lighter colours exhibit less absorption due to their higher reflectivity. The white paint surface absorbs the least at  $296\text{W/m}^2$  compared to Asphalt with the highest absorption factor of  $534\text{W/m}^2$ , all at the maximum sunlight (noon).

Given the above analyses, it is evident that the white colour materials are the best in terms of reflection and absorption of heat, while the black coloured materials are the worst. Yet the red bricks have medium values in both cases.

In Figure 9, the total annual reflected and absorbed energies for roofing and wall types have shown that metal roofing has the highest reflection energy with  $34108\text{J}$ , while dark concrete has the least reflection energy with  $4873\text{J}$ . But thatched roof has an equal amount of reflected and absorbed energies.

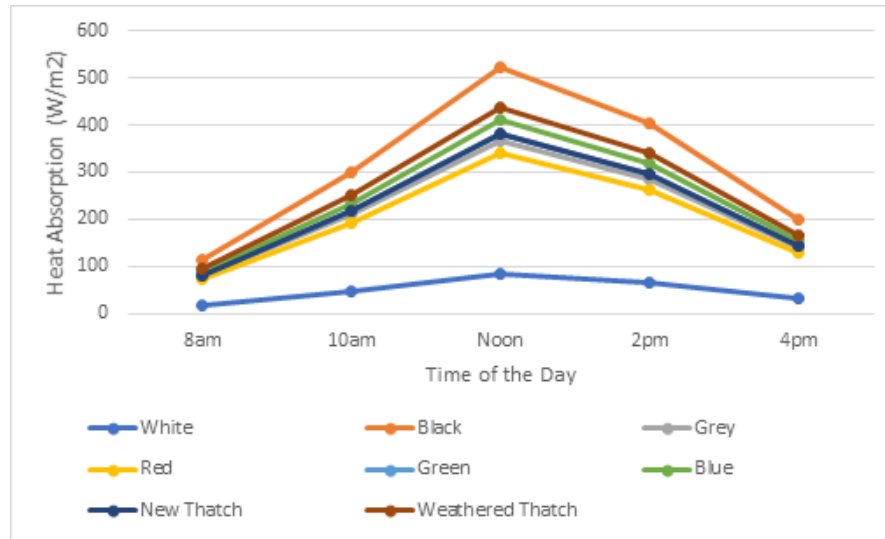


Figure 7: Heat Absorption Factor for Roofing Materials at Different Times of the Day

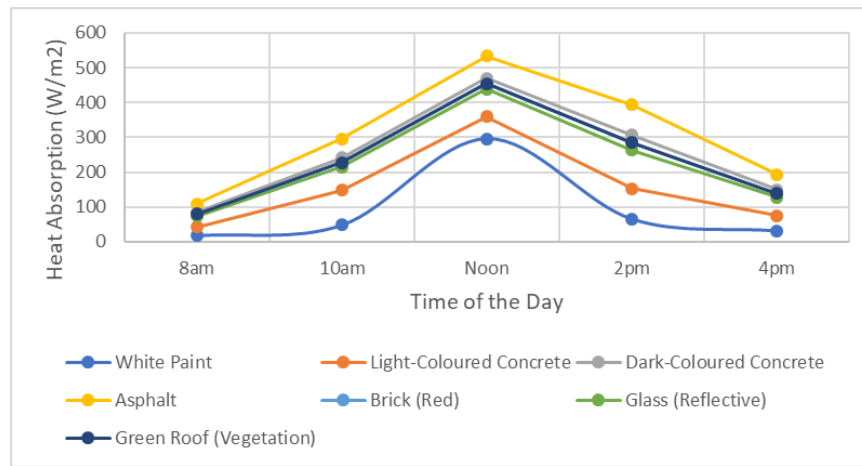


Fig. 8: Heat Absorption Factor for Building Materials at Different Times of the Day

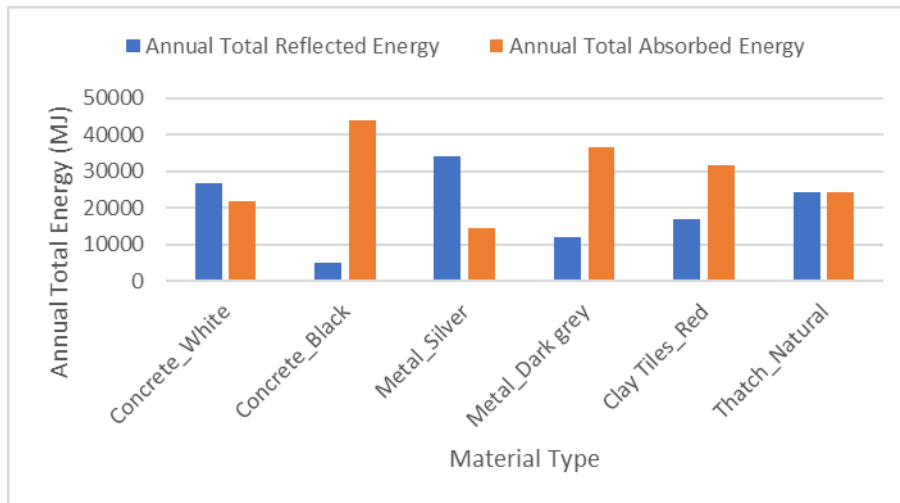


Fig. 9: Monthly Total Reflected Energy for Different Surfaces

### 4.3 Thermal Performance Analysis by Material

The temperature changes for the surface and the indoor environment based on monthly variation have shown the following results.

1. Dark Metal Roof has shown a very high surface material temperature rise of 10,667°C, showing extremely high heat absorption. Due to significant radiative heat gain that passes quickly into the building, the air temperature variation is found to be between 155 and 196°C presented in Figure 10. The indoor temperature change shows that June and July (with a wind speed of 2.9m/s) have the highest temperature rise of 196°C, and the lowest

values are found between September and December with  $155.6^{\circ}\text{C}$ . Therefore, dark metal roofs, even though they are a common, low-cost material they have high conductivity and, unless coated or insulated, are poor materials for heat conservation and comfort.

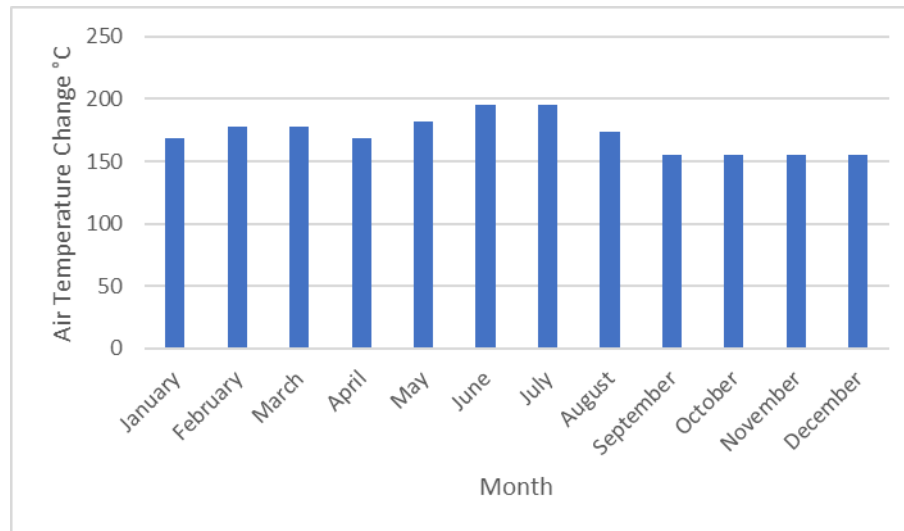


Fig. 10: Indoor Temperature Change of a Dark Metal Roof Material

2. Light Metal Roof has a material temperature absorption of  $4267^{\circ}\text{C}$  (a 60% reduction from the dark metal roof). The air temperature variation is found to be between  $110$  and  $142^{\circ}\text{C}$ . Therefore, changing the colour roof to lighter colours with higher reflection energy drastically reduced the temperature changes, thereby yielding significant thermal comfort.
3. Thatched Roof: This material has a material absorption temperature rise of  $67^{\circ}\text{C}$  and an indoor thermal temperature between  $2.2$  and  $3.4^{\circ}\text{C}$ . It has low conductivity and high specific heat, dampening peak temperatures. Thatched roofs are found to be better than metal roofs (though appearing less “modern”).
4. Concrete Wall: Despite absorbing high solar radiation performs as a thermal reservoir by absorbing heat slowly and releasing it over time. Therefore, if shaded or well-ventilated, they can be ideal for thermal stability

5. Brick Wall: This has a lower thermal conductivity and lower heat capacity as compared with concrete for indoor air moderation due to its lower heat capacity.

In Table 5, the summary of the monthly average for different materials is presented for material and indoor air temperature variations

Table 5: Summary for Building Material Calculated Temperature Variations

Material	$\Delta T_{material}(\text{°C})$	$\Delta T_{air} (\text{°C})$	Remarks
Dark Metal Roof	10,667	155 – 196	Very poor, high overheating risk
Light Metal Roof	4,267	110 – 142	Improved via high albedo
Thatched Roof	6.7	2.2 - 3.4	Low heat transfer, good insulation
Concrete wall	6.1	0.16 – 0.22	High thermal inertia, stable
Brick wall (Plastered)	5.3	0.18 -0.25	Efficient heat buffering

## 5.0 Conclusion

This study showed a simulation-based thermal analysis of some selected building materials commonly used in low-income housing in Kampala city of Uganda. The study considered monthly solar radiation data, wind speed, and material thermal properties. The surface temperature  $\Delta T_{material}$  and indoor air temperature rise  $\Delta T_{air}$  were quantified using monthly average sunshine hours exposure.

The results revealed a glaring difference between materials. It was seen that dark-coloured metal roofing, though common and affordable yet has extreme heat accumulation, making it unsuitable for thermally comfortable housing. To avert such a trend, light-coloured metal roofs showed a significantly reduced heat absorption of less than 60%, demonstrating a cost-effective improvement through simple colour change. However, using a thatched roof displayed the best

thermal performance, with low surface and indoor temperature rise owing to its low thermal conductivity and high specific heat, but it might be more susceptible to maintenance.

Concrete and brick walls provide stabilised indoor conditions due to their thermal mass and high specific heat, but they require good ventilation to avoid discomfort during the night as they retain heat. Therefore, the findings in the work showed the importance of context-specific passive design, especially in resource-constrained settings.

## Reference

A. Trlica, L. H. (2017). Albedo, land cover, and daytime surface temperature variation across an urbanized.

*Advancing Earth and Space Science*, 1-26.

Africa, B. V. (2023). *BiVA*. Retrieved from Uganda Energy Situation: [https://biovision-](https://biovision-africa.org/2023/04/07/uganda-energy-situation/?utm_source=chatgpt.com)

[africa.org/2023/04/07/uganda-energy-situation/?utm\\_source=chatgpt.com](https://biovision-africa.org/2023/04/07/uganda-energy-situation/?utm_source=chatgpt.com)

Biira, S. a. (2014). ANALYSIS OF SOLAR RADIATION IN UGANDA (A CASE STUDY OF KASESE, JINJA AND SOROTI DISTRICTS) . *Elsevier*, 8110-8115.

Climechart. (2024). *Kampala Climate Chart – Monthly Averages of Temperature and Rainfall*. Retrieved from

Climate Chart of Kampala, Uganda: <https://www.climechart.com/en/climate-chart/kampala/uganda>

Daniel N Katongole, K. N. (2023). Spatial and Temporal Solar Potential Variation Analysis in Uganda Using Measured Data. *Tanzania Journal of Science*, 1-14.

Elise Stull, X. S. (2010). Enhancing Urban Albedo to Fight Climate Change and Save Energy. *Sustainable Development law & policy*, 5-10.

Fuller, D. O., Roy, S. S., & Cohen, A. (2006). Land Surface Albedo of Large Urban Agglomerations from Landsat Observations. *American Geophysical Union, Joint Assembly, Baltimore, Maryland*.

Ian A. Smith, M. P. (2022). Urban green space and albedo impacts on surface temperature across seven United States cities. *Elsevier*, 1-44.

- K. W. Oleson, G. B. (2010). Effects of white roofs on urban temperature in a global climate model. *GEOPHYSICAL RESEARCH LETTERS*, 1 - 7.
- KasimI, O., AgbolaII, S., & Oweniwe, M. (2020). Land use land cover change and land surface emissivity in Ibadan, Nigeria. *Town and Regional Planning*.
- KCA. (2025, April). *Kampala Climate Change Action*. Retrieved from KCA, Kampala Climate Change Action, Energy and Climate Profile: <https://www.kcca.go.ug/>
- Kilama, S. B. (2014). ANALYSIS OF SOLAR RADIATION IN UGANDA (A CASE STUDY OF KASESE, JINJA AND SOROTI DISTRICTS). *International Journal of Current Research*, 1-7.
- Lei, M. Y. (2019). Deep learning in remote sensing applications: A meta-analysis and review. *ISPRS Journal of Photogrammetry and Remote Sensing*, 166 - 177.
- MA, H. T. (2023). Settlement Patterns and Environmental Adaptation in Settlement Patterns and Environmental Adaptation in Mountain Peninsula and West Mountain Island. *Soochow University*, 1-26.
- Masson-Delmotte, V. P. (2021). *Climate Change 2021: The Physical Science Basis*. IPCC.
- Mukwaya, H. E. (2021). *Kampala: City Scoping Study*. Kampala: African Cities Research Consortium.
- Nafees, M. (2024, November). *Role of albedo in adaptation to the effects of climate change and encourage everyone to participate in adaptation efforts*. Retrieved from researchgate.net: <https://www.researchgate.net/publication/386275016>
- NomadSeason. (2024). *Climate & UV Index in Kampala*. Retrieved from Monthly temperature, rainfall, and UV data, including variations in cloud cover and exposure risk.: <https://nomadseason.com/climate/uganda/central-region/kampala.html>
- Taha, H. (1997). Urban climates and heat islands: albedo, evapotranspiration, and anthropogenic heat. *Elsevier*, 99-103.

UBOS, U. B. (2024). *NATIONAL POPULATION AND HOUSING CENSUS 2024*. Kampala: NATIONAL POPULATION AND HOUSING CENSUS.

Xu, X., Gregory, J., & Kirchain, R. (2015). *THE IMPACTS OF SURFACE ALBEDO ON CLIMATE AND BUILDING ENERGY CONSUMPTION: REVIEW AND COMPARATIVE ANALYSIS*. TRB 2016 Annual Meeting.